Conformal Transformation of Linear Antenna Arrays through Transformation Optics

M. Salucci, G. Oliveri, N. Anselmi, and A. Massa

Abstract

In this work, an innovative Material-by-Design (*MbD*) methodology is proposed to address the conformal transformation of linear antenna arrays. A two-step quasi-conformal transformation optics (*QCTO*) is exploited in order to match the antenna onto arbitrary curved surfaces. Some preliminary numerical results are shown, obtained by means of full-wave simulations of the *MbD*-synthesized conformal radiating systems, in order to assess the effectiveness of the developed synthesis methodology.

1 Problem Formulation and Definitions

1.1 Transformation Description

1.1.1 Single Step TO

Each transformation involves two domains. In this report, the first domain is called "virtual domain" or "virtual space" while the other one is referred to as "physical domain" or "physical space". In addition, the terms "virtual" and "physical" are used to describe entities in virtual and physical spaces respectively. The rectangular coordinate system in virtual space is labeled as (x', y', z') whereas in the physical space the labels (x, y, z) are used. If the transformation from (x', y', z') to (x, y, z) is defined as:

$$(x, y, z) = \Gamma\left(x', y', z'\right) \tag{1}$$

$$x = x\left(x', y', z'\right) \tag{2}$$

$$y = y\left(x', y', z'\right) \tag{3}$$

$$z = z\left(x', y', z'\right) \tag{4}$$

the Jacobian matrix of the transformation $\underline{\underline{\Lambda}}$ will be:

$$\underline{\underline{\Lambda}} = \begin{bmatrix} \frac{\partial x}{\partial x'} & \frac{\partial x}{\partial y'} & \frac{\partial x}{\partial z'} \\ \frac{\partial y}{\partial x'} & \frac{\partial y}{\partial y'} & \frac{\partial y}{\partial z'} \\ \frac{\partial z}{\partial x'} & \frac{\partial z}{\partial y'} & \frac{\partial z}{\partial z'} \end{bmatrix}. \tag{5}$$

For the inverse transformation i.e. (x, y, z) to (x', y', z'),

$$\left(x', y', z'\right) = \Gamma'\left(x, y, z\right) \tag{6}$$

$$x' = x'\left(x, y, z\right) \tag{7}$$

$$y' = y'\left(x, y, z\right) \tag{8}$$

$$z' = z'\left(x, y, z\right) \tag{9}$$

the corresponding Jacobian matrix will be

$$\underline{\underline{\Lambda}}' = \begin{bmatrix} \frac{\partial x'}{\partial x} & \frac{\partial x'}{\partial y} & \frac{\partial x'}{\partial z} \\ \frac{\partial y'}{\partial x} & \frac{\partial y'}{\partial y} & \frac{\partial y'}{\partial z} \\ \frac{\partial z'}{\partial x} & \frac{\partial z'}{\partial y} & \frac{\partial z'}{\partial z} \end{bmatrix}. \tag{10}$$

and the following relations can be established.

$$\underline{\underline{\Lambda}}' = \underline{\underline{\Lambda}}^{-1} \tag{11}$$

$$det\left(\underline{\underline{\Lambda}}'\right) = \frac{1}{det\left(\underline{\underline{\Lambda}}\right)} \tag{12}$$

If $\underline{\underline{\varepsilon}}'$ and $\underline{\underline{\mu}}'$ represent permittivity and permeability tensors in virtual medium respectively,

$$\underline{\underline{\varepsilon}}' = \begin{bmatrix} \varepsilon'_{xx} & \varepsilon'_{xy} & \varepsilon'_{xz} \\ \varepsilon'_{yx} & \varepsilon'_{yy} & \varepsilon'_{yz} \\ \varepsilon'_{zx} & \varepsilon'_{zy} & \varepsilon'_{zz} \end{bmatrix} \tag{13}$$

$$\underline{\underline{\mu}}' = \begin{bmatrix} \mu'_{xx} & \mu'_{xy} & \mu'_{xz} \\ \mu'_{yx} & \mu'_{yy} & \mu'_{yz} \\ \mu'_{zx} & \mu'_{zy} & \mu'_{zz} \end{bmatrix} \tag{14}$$

corresponding permittivity and permeability tensors in physical space can be computed as follows:

$$\underline{\underline{\varepsilon}} = \frac{\underline{\underline{\Lambda}}\,\underline{\underline{\varepsilon}}'\,\underline{\underline{\Lambda}}^{T}}{det\left(\underline{\underline{\Lambda}}\right)} \tag{15}$$

$$\underline{\underline{\mu}} = \frac{\underline{\underline{\Lambda}}\,\underline{\underline{\mu}}'\,\underline{\underline{\Lambda}}^{T}}{det\left(\underline{\underline{\Lambda}}\right)}. \tag{16}$$

If there is a source with current I' and current density $\underline{J}'$ in virtual space its corresponding image in the physical space can be computed as

$$\underline{J} = \frac{\underline{\underline{\Lambda}}\,\underline{J}'}{det\left(\underline{\underline{\Lambda}}\right)}. \tag{17}$$

$$I = I'. \tag{18}$$

1.1.2 Two Step TO

For a cascade of transformations: $\widehat{\Gamma}\left\{(x', y', z') \rightarrow (x*, y*, z*)\right\}$ followed by $\widetilde{\Gamma}\left\{(x*, y*, z*) \rightarrow (x, y, z)\right\}$, the overall transformation $\Gamma\left\{(x', y', z') \rightarrow (x, y, z)\right\}$ can be formulated as follows. In the following discussion, and in the remaining of this report, when dealing with cascade of transformations, the space defined by the coordinates $(x*, y*, z*)$ will be termed as the *Intermediate* space and objects defined in this space will be called intermediate objects. Let $\widehat{\underline{\underline{\Lambda}}}$ and $\widetilde{\underline{\underline{\Lambda}}}$ represent the Jacobian matrices of the transformations $\widehat{\Gamma}$ and $\widetilde{\Gamma}$ respectively defined as:

$$\widehat{\underline{\underline{\Lambda}}} = \begin{bmatrix} \frac{\partial x*}{\partial x'} & \frac{\partial x*}{\partial y'} & \frac{\partial x*}{\partial z'} \\ \frac{\partial y*}{\partial x'} & \frac{\partial y*}{\partial y'} & \frac{\partial y*}{\partial z'} \\ \frac{\partial z*}{\partial x'} & \frac{\partial z*}{\partial y'} & \frac{\partial z*}{\partial z'} \end{bmatrix} \tag{19}$$

$$\underline{\underline{\widetilde{\Lambda}}} = \begin{bmatrix} \frac{\partial x}{\partial x*} & \frac{\partial x}{\partial y*} & \frac{\partial x}{\partial z*} \\ \frac{\partial y}{\partial x*} & \frac{\partial y}{\partial y*} & \frac{\partial y}{\partial z*} \\ \frac{\partial z}{\partial x*} & \frac{\partial z}{\partial y*} & \frac{\partial z}{\partial z*} \end{bmatrix}. \tag{20}$$

Further more, let $\left\{\underline{\underline{\varepsilon'}}, \underline{\underline{\mu'}}\right\}$, $\left\{\underline{\underline{\varepsilon*}}, \underline{\underline{\mu*}}\right\}$ and $\left\{\underline{\underline{\varepsilon}}, \underline{\underline{\mu}}\right\}$ represent sets of relative permittivity and permeability tensors in (x', y', z'), $(x*, y*, z*)$ and (x, y, z) spaces respectively, while the corresponding currents are represented as J', $J*$ and J. Considering the transformation: $\widetilde{\Gamma}\left\{(x*, y*, z*) \to (x, y, z)\right\}$, the following relations can be established:

$$\underline{\underline{\varepsilon}} = \frac{\underline{\underline{\widetilde{\Lambda}}}\,\underline{\underline{\varepsilon*}}\,\underline{\underline{\widetilde{\Lambda}}}^T}{det\left(\underline{\underline{\widetilde{\Lambda}}}\right)} \tag{21}$$

$$\underline{\underline{\mu}} = \frac{\underline{\underline{\widetilde{\Lambda}}}\,\underline{\underline{\mu*}}\,\underline{\underline{\widetilde{\Lambda}}}^T}{det\left(\underline{\underline{\widetilde{\Lambda}}}\right)} \tag{22}$$

and for the other transformation, $\widehat{\Gamma}\left\{(x', y', z') \to (x*, y*, z*)\right\}$,

$$\underline{\underline{\varepsilon*}} = \frac{\underline{\underline{\widehat{\Lambda}}}\,\underline{\underline{\varepsilon'}}\,\underline{\underline{\widehat{\Lambda}}}^T}{det\left(\underline{\underline{\widehat{\Lambda}}}\right)} \tag{23}$$

$$\underline{\underline{\mu*}} = \frac{\underline{\underline{\widehat{\Lambda}}}\,\underline{\underline{\mu'}}\,\underline{\underline{\widehat{\Lambda}}}^T}{det\left(\underline{\underline{\widehat{\Lambda}}}\right)}. \tag{24}$$

Substituting (23) and (24) in (21) and (22) respectively and rearranging terms gives the relationship between material properties for the overall transformation

$$\underline{\underline{\varepsilon}} = \frac{\left(\underline{\underline{\widetilde{\Lambda}\widehat{\Lambda}}}\right)\,\underline{\underline{\varepsilon'}}\,\left(\underline{\underline{\widetilde{\Lambda}\widehat{\Lambda}}}\right)^T}{det\left(\underline{\underline{\widetilde{\Lambda}\widehat{\Lambda}}}\right)} \tag{25}$$

$$\underline{\underline{\mu}} = \frac{\left(\underline{\underline{\widetilde{\Lambda}\widehat{\Lambda}}}\right)\,\underline{\underline{\mu'}}\,\left(\underline{\underline{\widetilde{\Lambda}\widehat{\Lambda}}}\right)^T}{det\left(\underline{\underline{\widetilde{\Lambda}\widehat{\Lambda}}}\right)}. \tag{26}$$

Following similar analysis, the current sources for the complete transformation can be related as:

$$\underline{J} = \frac{\left(\underline{\underline{\widetilde{\Lambda}\widehat{\Lambda}}}\right)\,\underline{J'}}{det\left(\underline{\underline{\widetilde{\Lambda}\widehat{\Lambda}}}\right)}. \tag{27}$$

$$I = I* = I'. \tag{28}$$

1.2 Isotropic Approximation

An isotropic approximation can be made on the permittivity and permeability of the medium (Lens) in the physical space under the following assumptions:

- TE or TM mode of propagation.
- Grid lines in virtual space are "near" orthogonal which results in a near-isotropic medium in virtual space.

Under such assumptions, permittivity and permeability in physical space will be simplified as:

- For TE mode of propagation:
  - Approximate Isotropic permeability: $\underline{\underline{\mu}}^{approx.} = \mu^{approx.}\mathbb{I}$;
  - Constant Approximate permittivity: $\underline{\underline{\varepsilon}}^{approx.} = \mathbb{I}$;
- For TM mode of propagation:
  - Approximate Isotropic permittivity: $\underline{\underline{\varepsilon}}^{approx.} = \varepsilon^{approx.}\mathbb{I}$;
  - Constant Approximate permeability: $\underline{\underline{\mu}}^{approx.} = \mathbb{I}$;

where $\mathbb{I}$ is a 3×3 identity matrix, $\varepsilon^{approx.}$ and $\mu^{approx.}$ are computed by ratio of areas of virtual and physical transformation grid cells. More specifically, for a given unit cell in the physical space, if its area is approximated by $A^{physical} = \Delta x \Delta y$, where Δx and Δy are changes in x and y between its opposite corners, and similarly if the area of the image of this unit cell in virtual space can be approximated by $A^{virtual} = \Delta x' \Delta y'$, the approximate permittivity or permeability of the unit cell is computed as: $\frac{A^{virtual}}{A^{physical}} = \frac{\Delta x' \Delta y'}{\Delta x \Delta y}$.

- For TE mode of propagation:

$$\mu^{approx.} = \frac{A^{virtual}}{A^{physical}} = \frac{\Delta x' \Delta y'}{\Delta x \Delta y} \tag{29}$$

- For TM mode of propagation:

$$\varepsilon^{approx.} = \frac{A^{virtual}}{A^{physical}} = \frac{\Delta x' \Delta y'}{\Delta x \Delta y} \tag{30}$$

1.3 Transformation Grid Orthogonality (χ)

Since the orthogonality of the transformation grid is the basis for isotropic approximation, it is quantified as follows. Figure 1 shows a sample grid intersection in the complex plane $\gamma = x + jy$.

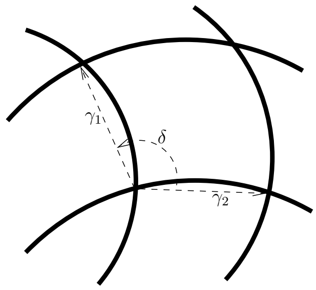

Figure 1: Description of grid orthogonality measure: A sample unit cell of a grid in the complex plane

Referring to Figure 1, and using Euler's notation, $\gamma_1 = |\gamma_1|\, e^{j[arg(\gamma_1)]}$, $\gamma_2 = |\gamma_2|\, e^{j[arg(\gamma_2)]}$, where γ_1 and γ_2 are vectors forming adjacent sides of the unit cell. The internal angle δ can be computed as

$$\delta = arg\,(\gamma_1) - arg\,(\gamma_2) = arg\left(\frac{\gamma_1}{\gamma_2}\right).$$

The offset from orthogonality χ can then be evaluated as

$$\chi = \delta - 90. \tag{31}$$

1.4 Field Matching Error (ξ)

The error between a given field distribution E and a reference field distribution E_{ref} sampled at U and V points in the x and y directions respectively (i.e $x_u \in \{x_1, \cdots, x_U\}$, $y_v \in \{y_1, \cdots, y_V\}$) is evaluated as:

$$\xi = \frac{\sum_{u=1}^{U}\sum_{v=1,(x_u,y_v)\notin\Theta}^{V} \left|E_{ref}\,(x_u, y_v) - E\,(x_u, y_v)\right|}{\sum_{u=1}^{U}\sum_{v=1,(x_u,y_v)\notin\Theta}^{V} \left|E_{ref}\,(x_u, y_v)\right|} \tag{32}$$

where Θ represents an area excluded from the evaluation. This expression is typically used to evaluate the difference between fields radiated from a reference virtual array and an array enhanced by metamaterial lens, where the comparison is made outside the lens region (i.e., Θ is the boundary of the synthesized lens).

1.5 Anisotropy Measures

- Maximum lens permittivity

$$\max\left\{\underline{\underline{\varepsilon}}\right\} = \max_{\mathbf{r}\in\Omega}\left\{\varepsilon_{pq}\left(\mathbf{r}\right); \, p,q \in \{1,2,3\}\right\}$$

- Minimum lens permittivity

$$\min\left\{\underline{\underline{\varepsilon}}\right\} = \min_{\mathbf{r}\in\Omega}\left\{\varepsilon_{pq}\left(\mathbf{r}\right); \, p,q \in \{1,2,3\}\right\}$$

- Average fractional anisotropy

$$\alpha_F = \frac{1}{area\left(\Omega\right)}\int_{\mathbf{r}\in\Omega}\sqrt{\frac{3\sum_{i=1}^{3}\left[\sigma_i\left(\mathbf{r}\right)-\sigma_{ave}\left(\mathbf{r}\right)\right]^2}{2\sum_{i=1}^{3}\left[\sigma_i\left(\mathbf{r}\right)\right]^2}}d\mathbf{r}$$

- Average relative anisotropy

$$\alpha_R = \frac{1}{area\left(\Omega\right)}\int_{\mathbf{r}\in\Omega}\sqrt{\frac{\sum_{i=1}^{3}\left[\sigma_i\left(\mathbf{r}\right)-\sigma_{ave}\left(\mathbf{r}\right)\right]^2}{3\sigma_{ave}\left(\mathbf{r}\right)}}d\mathbf{r}$$

Where

- $\sigma_i\left(\mathbf{r}\right)$, $i = 1, ..., 3$ are the eigenvalues of the permittivity tensor $\underline{\underline{\varepsilon}}\left(\mathbf{r}\right)$;
- $\sigma_{ave}\left(\mathbf{r}\right) = \frac{\sum_{i=1}^{3}\sigma_i(\mathbf{r})}{3}$ is the average of the eigenvalues;
- Ω is the external perimeter of the lens.

2 Preliminary Assessment

2.1 Conf. #1 - Preliminary Transformation Test (No SI)

Input Parameters

- **Virtual & Physical Geometries**

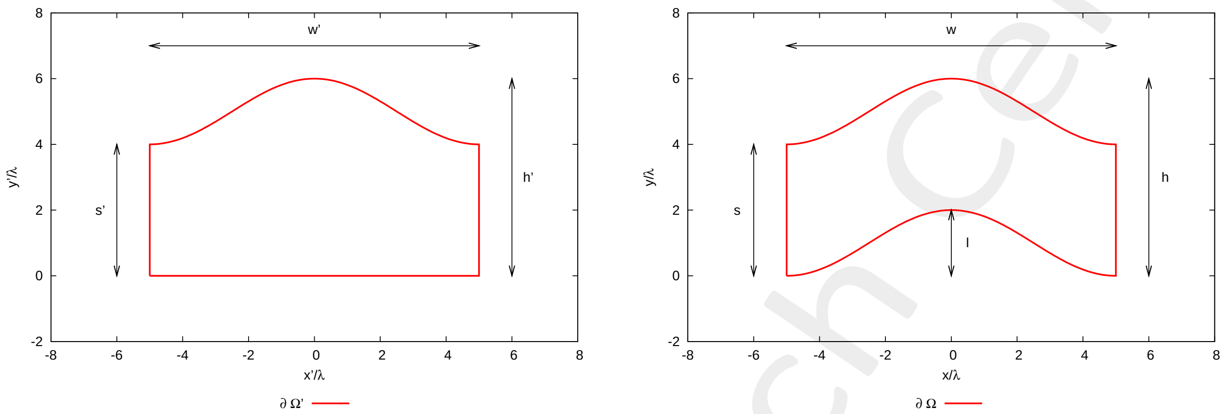

(a) (b)

Figure 2: Transformation regions and geometric parameters of interest.

Virtual				Physical			
w' [λ]	h' [λ]	s' [λ]	l' [λ]	w [λ]	h [λ]	s [λ]	l [λ]
16.0	4.5	4.0	0.0	16.0	4.5	4.0	0.5

Table I: Geometric descriptors for virtual and physical geometries.

- **Virtual Array**
  - Number of elements, spacing, aperture: $N' = 20$, $d' = \frac{\lambda}{2}$, $L' = 9.5$ [λ];
  - Distance from PEC ground plane (placed at $y' = 0.0$): $\delta' = \frac{\lambda}{4}$;
  - Operating frequency: $f = 600$ [MHz];
  - Steering angle: $\phi_s = 90.0$ [deg];
  - Excitations: $I_n = 1.0$, $\varphi_n = \frac{-2\pi}{\lambda} x_n sin\left(\phi_s + 90\right)$; $n = 1, ..., N'$;
- **QCTO**
  - Discretization cell dimension: 0.15 [λ] (0.01 [λ] for source mapping);

2.1.1 Results of the Transformation

Transformation Grids

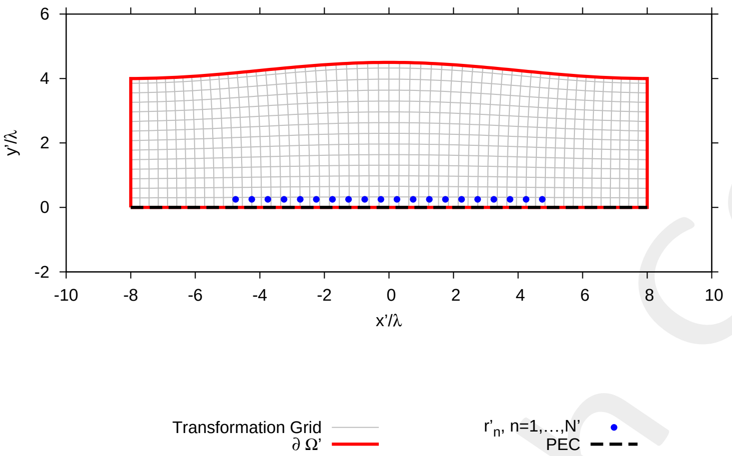

(a) Virtual

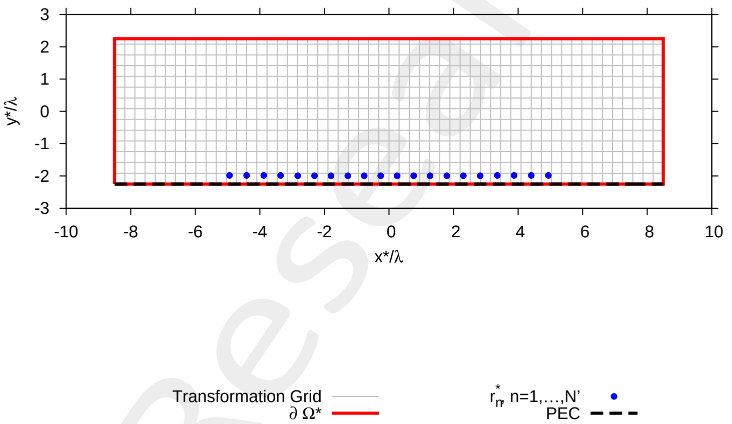

(b) Intermediate

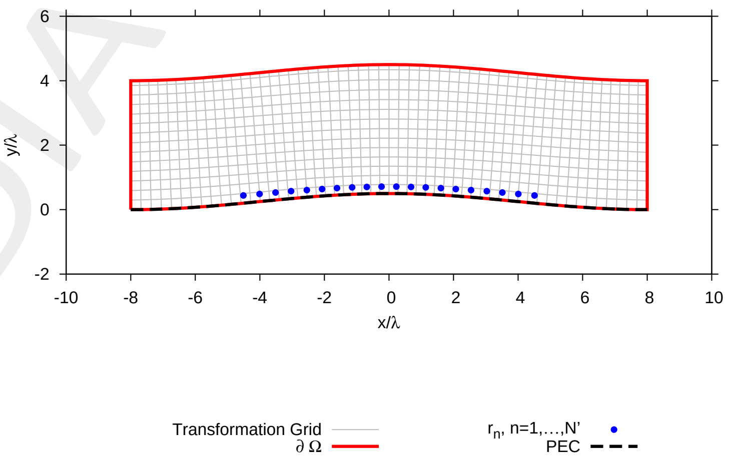

(c) Physical

Figure 3: Transformation grids for (a) virtual (b) intermediate and (c) physical geometries.

Physical Lens Permittivity Tensor

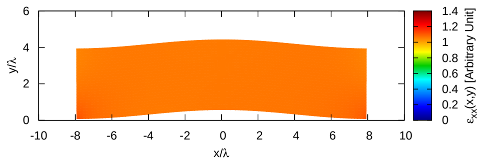

$(a)\ \varepsilon_{xx}$

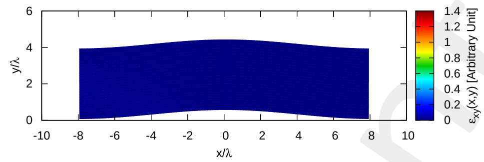

$(b)\ \varepsilon_{xy}$

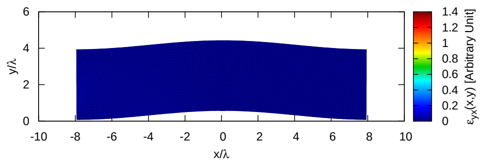

$(c)\ \varepsilon_{yx}$

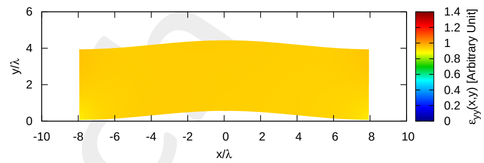

$(d)\ \varepsilon_{yy}$

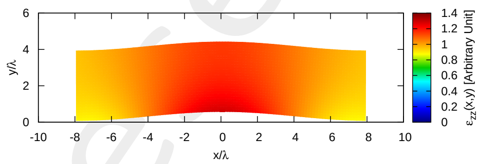

$(e)\ \varepsilon_{zz}$

Figure 4: Components of the relative permittivity tensor of the lens.

Physical Lens Isotropic Approximation

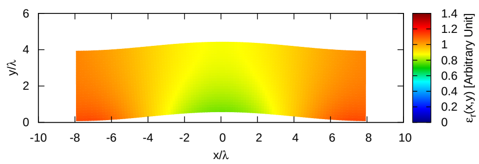

Figure 5: Isotropic approximate permittivity distribution of the lens.

Grid Orthogonality

Virtual **Physical**

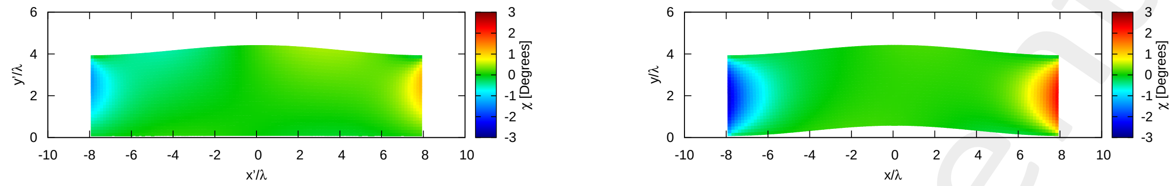

(a) (b)

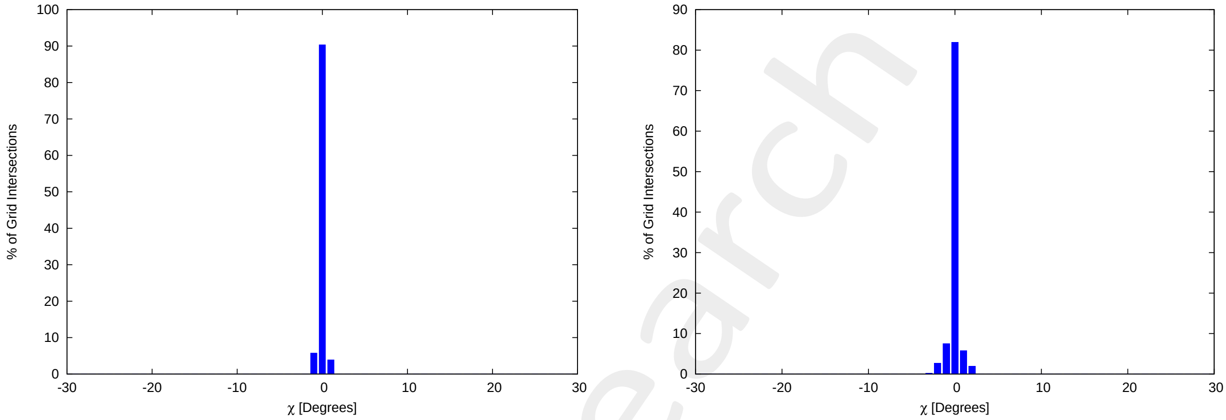

(c) (d)

Figure 6: Orthogonality of the virtual and physical grids.

2.1.2 Near-Field Distributions

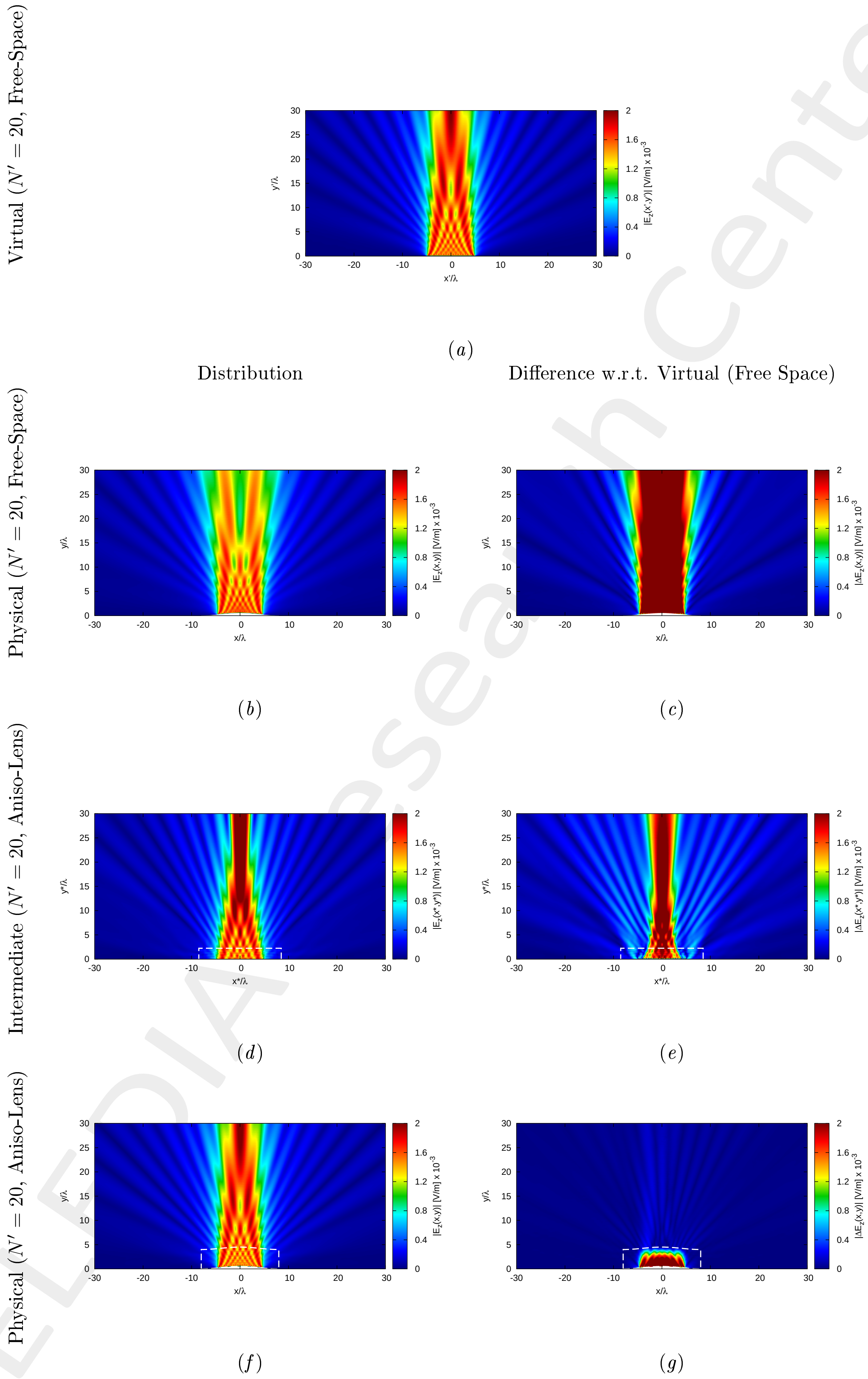

Figure 7: Electric field distributions.

2.1.3 Far-Field Patterns

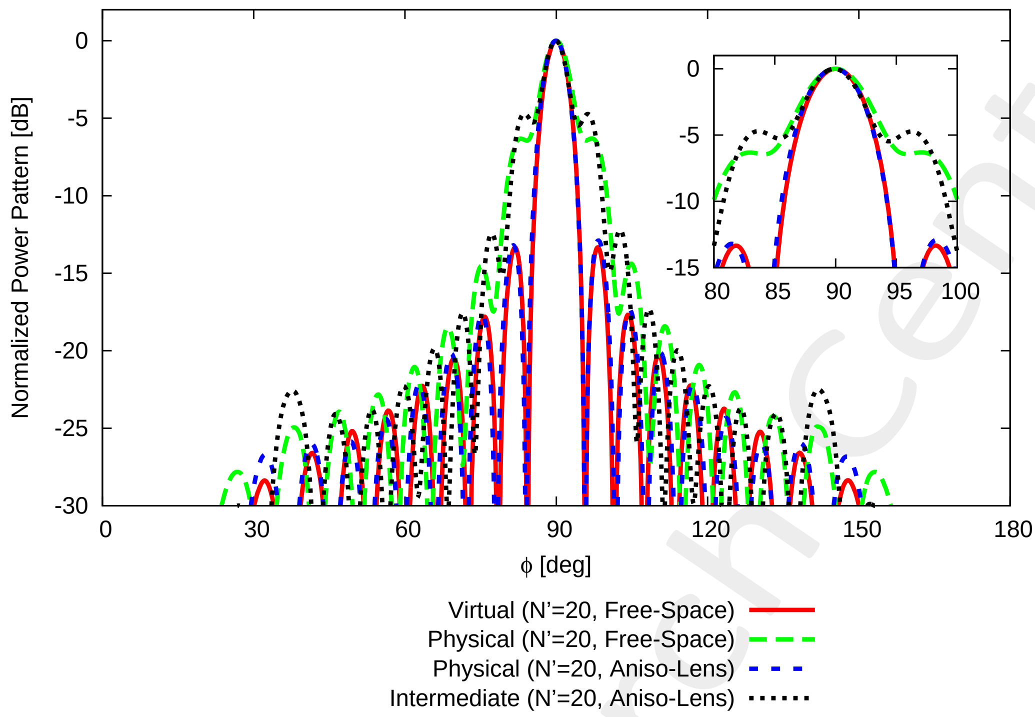

Figure 8: Comparison between normalized power patterns.

2.1.4 Summary

Intermediate Lens	
Height	4.5 [λ]
Width	17.0 [λ]
Anisotropic Permittivity Range	$[-0.02, 1.09]$
Isotropic Permittivity Range	$[0.75, 1.09]$
Physical Lens	
Anisotropic Permittivity Range	$[-0.03, 1.29]$
Isotropic Permittivity Range	$[0.77, 1.13]$

Table II: Transformation statistics.

	Virtual Array	Intermediate Array		Physical Array		
Environment	Free-Space	Aniso-Lens	Iso-Lens	Free-Space	Aniso-Lens	Iso-Lens
Number of elements	20	20		20		
Aperture on x [λ]	9.5	9.88		9.02		
Aperture on y [λ]	0.0	0.01		0.27		
Aperture Ratio on x, $\rho_x = \frac{\{L*,L\}}{L'}$	-	1.04		0.95		
$SLL[dB]$	13.12	4.70		6.30	12.89	
$FNBW$ [deg]	11.43	9.00		11.70	11.70	
$3dB$ Beamwidth [deg]	5.09	5.30		6.11	5.19	

Table III: Summary.

References

[1] G. Oliveri, G. Gottardi, F. Robol, A. Polo, L. Poli, M. Salucci, M. Chuan, C. Massagrande, P. Vinetti, M. Mattivi, R. Lombardi, and A. Massa, "Co-design of unconventional array architectures and antenna elements for 5G base station," *IEEE Trans. Antennas Propag.*, vol. 65, no. 12, pp. 6752-6767, Dec. 2017.

[2] P. Rocca, G. Oliveri, R. J. Mailloux, and A. Massa, "Unconventional phased array architectures and design methodologies - A review," *Proc. IEEE*, vol. 104, no. 3, pp. 544-560, Mar. 2016.

[3] G. Oliveri, M. Salucci, N. Anselmi and A. Massa, "Multiscale System-by-Design synthesis of printed WAIMs for waveguide array enhancement," *IEEE J. Multiscale Multiphysics Computat. Techn.*, vol. 2, pp. 84-96, 2017.

[4] A. Massa and G. Oliveri, "Metamaterial-by-Design: Theory, methods, and applications to communications and sensing - Editorial," *EPJ Applied Metamaterials*, vol. 3, no. E1, pp. 1-3, 2016.

[5] L. Poli, G. Oliveri, P. Rocca, M. Salucci, and A. Massa, "Long-Distance WPT Unconventional Arrays Synthesis," *J. Electromagnet. Waves Appl.*, vol. 31, no. 14, pp. 1399-1420, Jul. 2017.

[6] G. Oliveri, F. Viani, N. Anselmi, and A. Massa, "Synthesis of multi-layer WAIM coatings for planar phased arrays within the system-by-design framework," *IEEE Trans. Antennas Propag.*, vol. 63, no. 6, pp. 2482-2496, Jun. 2015.

[7] G. Oliveri, L. Tenuti, E. Bekele, M. Carlin, and A. Massa, "An SbD-QCTO approach to the synthesis of isotropic metamaterial lenses," *IEEE Antennas Wireless Propag. Lett.*, vol. 13, pp. 1783-1786, 2014.

[8] G. Oliveri, D. H. Werner, and A. Massa, "Reconfigurable electromagnetics through metamaterials - A review" *Proc. IEEE*, vol. 103, no. 7, pp. 1034-1056, Jul. 2015.

[9] G. Oliveri, E. T. Bekele, M. Salucci, and A. Massa, "Transformation electromagnetics miniaturization of sectoral and conical horn antennas," *IEEE Trans. Antennas Propag.*, vol. 64, no. 4, pp. 1508-1513, Apr. 2016.

[10] G. Oliveri, E. T. Bekele, M. Salucci, and A. Massa, "Array miniaturization through QCTO-SI metamaterial radomes," *IEEE Trans. Antennas Propag.*, vol. 63, no. 8, pp. 3465-3476, Aug. 2015.

[11] G. Oliveri, E. T. Bekele, D. H. Werner, J. P. Turpin, and A. Massa, "Generalized QCTO for metamaterial-lens-coated conformal arrays," *IEEE Trans. Antennas Propag.*, vol. 62, no. 8, pp 4089-4095, Aug. 2014.

[12] G. Oliveri, E. Bekele, M. Carlin, L. Tenuti, J. Turpin, D. H. Werner, and A. Massa, "Extended QCTO for innovative antenna system designs," IEEE Antenna Conference on Antenna Measurements and Applications (CAMA 2014), pp. 1-3, Nov. 16-19, 2014.

[13] G. Oliveri, P. Rocca, M. Salucci, E. T. Bekele, D. H. Werner, and A. Massa, "Design and synthesis of innovative metamaterial-enhanced arrays," IEEE International Symposium on Antennas Propag. (APS/URSI 2013), Orlando, Florida, USA, pp. 972 - 973, Jul. 7-12, 2013.

[14] G. Oliveri, "Improving the reliability of frequency domain simulators in the presence of homogeneous metamaterials - A preliminary numerical assessment," *Progress In Electromagnetics Research*, vol. 122, pp. 497-518, 2012.

[15] M. Salucci, G. Oliveri, N. Anselmi, G. Gottardi, and A. Massa, "Performance enhancement of linear active electronically-scanned arrays by means of MbD-synthesized metalenses," *J. Electromagnet. Waves Appl.*, vol. 32, no. 8, pp. 927-955, 2018.

[16] M. Salucci, G. Oliveri, N. Anselmi, and A. Massa, "Material-by-design synthesis of conformal miniaturized linear phased arrays," *IEEE Access* (doi: 10.1109/ACCESS.2018.2833199).